# Efficient Thermal Electric Skipping Strategy applied to the Control of Series/Parallel Hybrid Powertrain

**Author, co-author (Do NOT enter this information. It will be pulled from participant tab in MyTechZone)**

Affiliation (Do NOT enter this information. It will be pulled from participant tab in MyTechZone)

## Abstract

The optimal control of hybrid powertrains represents one of the most challenging tasks for the compliance with the legislation concerning $CO_2$ and pollutant emission of vehicles. Most common off-line optimization strategies (Pontryagin minimum principle – PMP – or dynamic programming) allow to identify the optimal control along a predefined driving mission at the expense of a quite relevant computational effort. On-line strategies, suitable for on-vehicle implementation, involve a certain performance degradation depending on their degree of simplification and computational effort.

In this work, a simplified control strategy is presented, where the conventional power-split logics, typical of the above-mentioned strategies, is here replaced with an alternative utilization of the thermal and electric units for the vehicle driving (Efficient Thermal Electric Skipping Strategy - ETESS). The choice between the units is realized at each time and is based on the comparison between the effective fuel rate of the thermal engine and an equivalent fuel rate related to the electrical power consumption. The equivalent fuel rate in a pure electric driving is associated to a combination of brake specific fuel consumption of the thermal engine, and electro-mechanical efficiencies along the driveline.

The ETESS is applied for the simulation of segment C hybrid vehicle, equipped with a thermal engine and two electric units (motor and generator). The methodology is tested along regulatory driving cycles (WLTP, Artemis) and RDE, with different powertrain variants. Numerical results underline that the proposed approach performs very close to most common control strategies (consumed fuel per kilometer higher than PMP of about 1% on average). The main advantage is a reduced computational effort (decrease of 99% on average). The ETESS is straightforwardly adapted for an on-line implementation, through the introduction of an adaptive factor, preserving the computational effort and the fuel economy.

## Introduction

The development of Hybrid Electric Vehicles (HEVs) is continuously increasing due to the demonstrated capability to reduce the $CO_2$ emissions compared to conventional vehicles [1]. This result is achieved at the expense of a more complex control strategy of the powertrain. This last is composed of a thermal unit (Internal Combustion Engine - ICE), which is coupled in series and/or parallel to one or more electric units, linked to an energy storage device, usually a battery [2]. Whatever is the hybrid architecture, the control strategy has the role to identify the optimal power to be

delivered/absorbed by the available units, once assigned the power demand at the vehicle wheels. The main objective of the control system is to minimize fuel consumption along a route, rather than to decrease the fuel flow rate at each instant of time.

Most common hybrid powertrains present a parallel disposition of the ICE and of an Electric Motor (EM) and, in these cases, the control problem consists of the identification at each time of the power-split between the units. The introduction of a second electric unit (Electric Generator - EG), connected in series to the thermal engine, allows for a more flexible and efficient handling of the battery charging phases, allowed also when the vehicle is stationary. Numerous optimization logics have been proposed for HEV to maximize the fuel economy.

As a reference approach, the Dynamic Programming (DP) method [3] numerically solves the problem to find global optimal behavior on the basis of the complete topology and speed profile of a driving scenario [4]. This methodology is highly time-demanding and cannot be directly applied in a real-time implementation, requiring information about future events. As well as other methods, due to *a-priori* knowledge of future information, the DP is classified as a Global Optimization Strategy (GOS). The DP can be successfully applied in the design phase of a new powertrain architecture and could give useful indications for the definition of heuristic strategies [5]. To address the lack for future event, the stochastic DP algorithm was proposed by establishing driver power demand sequence over different driving cycles based on Markov chain [6]. However, this DP variant still suffers from computational issue for a real-time implementation.

As an alternative approach, conventional analytical optimization methods can be applied for the optimization problem of HEV energy management, such as the Pontryagin Minimum Principle (PMP) [7]. It is based on the instantaneous minimization of the Hamiltonian function, once determined the optimal trajectory of the costate. To realize the condition of energy balance for the battery, the knowledge of the driving mission is mandatory.

A critical issue of these approaches is the discretization of the operating domain of the powertrain components, which depends on the conflicting demands of computational effort and fine control.

The above strategies can be extended for an-online application, solving the issue concerning lack of information about future events. A very common approach is the Equivalent Consumption Minimization Strategy (ECMS) [8], which can be considered an extension of the PMP [9]. It is based on the on-line minimization of an equivalent fuel consumption, also accounting for a contribution

related to the battery power consumption through an equivalence factor, $s_0$. The suitability for on-line implementations is realized by an adaptive $s_0$, adjusted by a Fuzzy PI controller [10] or by a correction term depending on the battery State of Charge (SoC) [11]. Once tuned, these approaches proved sub-optimal performance, but quite similar to off-line approaches [12,13]. Once again, the computational time may represent an issue, if a refined discretization for the exploration of the performance maps of powertrain sub-components is required.

Based on the above considerations, the main aim of this work is the development of a simplified control strategy, very efficient from a computational viewpoint, but, at the same time, with performance similar to PMP/ECMS. The power-split principle is not applied, replaced by an alternate utilization of thermal and electric units (Efficient Thermal Electric Skipping Strategy - ETESS). At each time, the choice between the traction modality depends on the evaluation of an equivalent fuel rate in a pure electric driving, to be compared to actual fuel rate in a pure ICE driving. The ETESS is implemented in an "in-house developed" simulation platform and applied to a reference C segment vehicle along different driving missions, with some powertrain variants. After a description of the tested HEV architecture and features, the ETESS is detailed. Finally, the results of the proposed control strategy are discussed and compared, in off-line and on-line variants, to PMP and ECMS approaches, respectively.

## HEV Architecture

The vehicle investigated in this work is a HEV, belonging to the C segment. Its main characteristics are listed in Table 1 [14]. It presents a combined parallel/series powertrain, which is schematized in Figure 1. The powertrain is composed of an ICE, two Electric Motor/Generator units, (EM and EG), a battery (Ba), three clutches (Cl$_{1-3}$) and two Gear-Boxes (GB$_{1-2}$). This architecture favours a flexible control of its components, thanks to the presence of the three clutches. Moreover, they contribute to minimize the mechanical losses when one of the motors is not used, avoiding load-less operations.

Two modes, namely series and parallel modes, are available when a tractive demand is requested to the powertrain. In the series modality, the vehicle is moved by the EM. Two sub-states are available: pure electric driving and charging in series mode. In this case, the ICE, decoupled from the wheels, charges the battery through the EG. Concerning the parallel modality, the power demand is fulfilled by ICE and EM, either in a combined manner (power-split concept) or by only one of them. In parallel mode, the charging is allowed but, in this case, the ICE operating condition depends on the current vehicle speed. The regenerative breaking is realized by EM, supported by the EG if necessary.

This work concerns a prototype vehicle, equipped with a very efficient ICE still under development [15]. The main characteristic of this engine is to operate with an ultra-lean combustion, leading to very high efficiencies over the whole operating domain. The model-estimated BSFC map of the tested engine is plotted in Figure 2. The latter also depicts an intermediate dashed line, corresponding to a smaller engine with a halved rated torque.
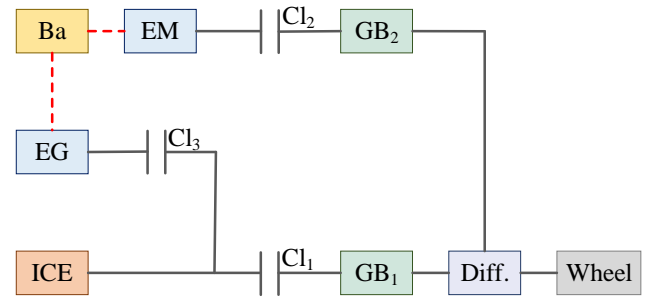


Figure 1. Powertrain schematic of the tested HEV.

Table 1. Main characteristics of the tested HEV.

| Hybrid Electric Vehicle Features | |
| --- | --- |
| Vehicle | |
| Mass, kg | 1730 |
| Car aero drag, m$^2$ | 0.775 |
| Tire rolling resistance coeff., - | 0.008 |
| Wheel diameter, m | 0.723 |
| Axle ratio, - | 4.4 |
| Axle inertia, kgm$^2$ | 1.5 |
| Internal Combustion Engine | |
| Displacement, cm$^3$ | 1633.1 |
| Max Power, kW | 125 |
| Inertia, kgm$^2$ | 0.35 |
| Electric Motor | |
| Max Power, kW | 55 |
| Max Torque, Nm | 165 |
| Inertia, kgm$^2$ | 0.10 |
| Electric Generator | |
| Max Power, kW | 50 |
| Max Torque, Nm | 240 |
| Inertia, kgm$^2$ | 0.10 |
| Battery | |
| Internal Resistance, Ohm | 0.375 |
| Voltage, Volt | 400.0 |
| Energy density, Wh/kg | 170.0 |
| Usable battery sizing, kWh | 0.50 |
| SoC limits, - | $0.2 - 0.9$ |
| Gear-Box$_1$ | |
| Gear 1 Ratio, - | 2.72 |
| Gear 2 Ratio, - | 1.64 |
| Gear 3 Ratio, - | 0.99 |
| Gear 4 Ratio, - | 0.60 |
| Gear-Box$_2$ | |
| Gear 1 Ratio, - | 2.67 |
| Gear 2 Ratio, - | 1.03 |
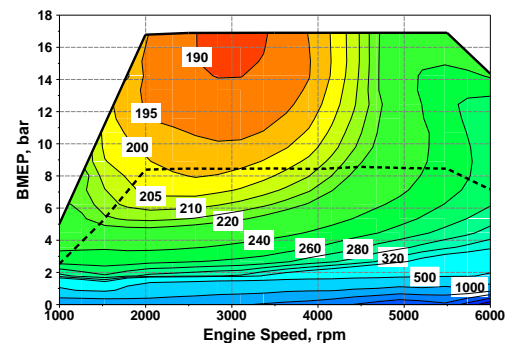


Figure 2. Thermal engine BSFC map (g/kWh).

## Simulation Platform

The vehicle simulations are carried out by a "in-house developed" software, implemented in Fortran language (UniNa Vehicle Simulation - UNVS). It is based on a "forward kinematic" approach [16]. Each component of the powertrain schematic in Figure 1 is described by a lumped-parameter approach. The tractive demand at the wheels considers the inertial forces (related to vehicle and rotating parts), resistances (aerodynamic and rolling load) and road grade. The thermal unit is characterized by a quasi-steady map-based approach. In particular, the BSFC map is implemented, collecting the BSFC levels as a function of the engine BMEP and speed, together with the maximum shaft torque curve. For both electric units, the maximum and minimum shaft torque curves are assigned. Their efficiencies could be described by a map-based approach (dependent on speed and torque), but in this study they are assumed constants. The battery is treated by a conventional SoC model, which calculates the current SoC based on the electric flux absorbed from or supplied to the battery [9]. An internal resistance is imposed to estimate the Joule-effect losses. No resistance variation is considered at changing SoC and temperature. The mechanical losses in the gearboxes are evaluated assuming constant efficiencies.

A linear interpolation method is used to access the map of BSFC and the torque constraint curves. The fuel consumption at zero or negative load is estimated by a torque-dependent linear extrapolation method, following the observations in [17]. The effects of the ICE thermal transient are not considered in the simulations, resulting a null fuel consumption penalization at cold start. It is worth to underline that the main aim of the proposed work is not to propose a detailed vehicle simulator, but to illustrate the potential of the proposed powertrain control strategy. Hence, the adopted simplified modeling can be considered reliable enough to get the above-mentioned aim.

The consistency of the physics behind the simulation platform has been verified in preliminary calculations with reference to segment C vehicles, driven by a conventional powertrain and a current state-of-art commercial SI engine. Simulations are carried out along a NEDC, for which the numerical findings in terms of grams of fuel per kilometer underestimated the experimental datum, with a difference of 3.5%. This disagreement could be partially explained by having neglected the ICE cold start, as highlighted by experimental evidences [18]. Detailed results cannot be proposed due to confidentiality reasons. The simulation results are assumed satisfactory, considering that the main aim of the presented work is, as stated above, the comparison between powertrain control strategies, rather than a sophisticate description of all the phenomena occurring in a vehicle and in its powertrain.

## State of Art for Hybrid Powertrain Management Strategy

The aim of whatever control strategy for the vehicle powertrain is the minimization of predefined quantities, for instance, the consumed fuel or the pollutant emission along a driving mission, complying with some constraints, for instance, the maximum or minimum engine torque or rotational speed, etc. To simplify the process, in most cases, the minimization concerns a combination of the above quantities, leading to the following mathematical formulation of the problem:

$$\arg\min_{u(t)} J\big[x(t),t\big]$$
$$u(t) \in U \tag{1}$$
$$x(t) \in X$$

where $J$ is the so-called performance index to minimize, $x$ is the generic state variable and $u$ is the generic control variable, and $X$ and $U$ the related range of variation. $J$ depends on the integral of a cost function $L$ from $t$ to $t_0$ and on the difference between the current and the initial state variable, through the penalization factor $\beta$.

$$J\big[x(t),t\big] = \int_{t_0}^{t} L\big[x(t),u(t),t\big]dt + \beta\big(x(t_0)-x(t)\big) \tag{2}$$

Under the common hypothesis that the quantity to minimize is the consumed fuel along the driving cycle, the only state variable is the battery SoC, and the control variable is the power-split between thermal engine and electric units ($u=P_{el}/P_{dem}$), the cost function writes:

$$J\big[x(t),t\big] = \int_{t_0}^{t} \dot{m}_f\big[u(t),t\big]dt + \beta\big(SoC(t_0)-SoC(t)\big) \tag{3}$$

The second term on the right hand of Eq. (3) can be considered as a global constraint, required by the vehicle certification process for the energy-storage system.

The PMP indicates that the optimal solution can be found at each time by minimizing the Hamiltonian:

$$H\big[u(t),SoC(t),t,\lambda(t)\big] = $$
$$\dot{m}_f\big[u(t),t\big] + \lambda(t)\dot{SoC}\big[u(t),SoC(t),t\big] \tag{4}$$

where $\lambda(t)$ is the so-called costate. Its dynamic equation is expressed by:

$$\dot{\lambda}(t) = -\frac{H\big[u(t),SoC(t),\lambda(t),t\big]}{\partial SoC} = $$
$$-\lambda(t)\frac{\partial \dot{SoC}\big[u(t),SoC(t),t\big]}{\partial SoC} \tag{5}$$

Based on the common assumption of not-dependence of the SoC time derivative on its current level [9], the costate is constant over time, and the optimal costate, labelled as $\lambda^*$, has only to satisfy the energy balance for the battery between the beginning and the end of the driving cycle:

$$SoC(t_0) = SoC(t_f) \tag{6}$$

The identification of $\lambda^*$ can be realized only when the vehicle driving mission is defined "a priori", relaying on the knowledge of future information.

When the Hamiltonian cannot be expressed as an explicit function of the control variable, the solution of the problem requires a discretization of the control variable domain at each simulation step. Depending on the grid sizing, the problem solution may change, leading to quite different results in terms of cost function minimum and control variable trajectory. Finer grids determine better results, but the computational time may become an issue.

The ECMS can be considered as an on-line variant of the PMP [9]. In this case, the methodology involves the minimization at each time of an equivalent fuel rate, sum of the actual fuel rate and a contribution related to the electrical power through an equivalence factor, according to:

$$\dot{m}_{eq}\left[u(t),t\right] = \dot{m}_f\left[u(t),t\right] + s_0 \frac{P_{bat}\left[u(t),t\right]}{LHV} \qquad (7)$$

*LHV* being the low heating value of the fuel, $P_{bat}$ the power delivered or drained by the battery and $s_0$ an equivalence factor. A piecewise linear type description of $s_0$ (differentiated between battery charge and discharge phases) proved to perform very close to the optimal powertrain management, but needs to be adjusted according to the vehicle characteristics and driving mission [13]. Various approaches were proposed to realize an adaptative adjustment of the equivalence factor [10, 11, 13]. Some of them are informed on the basis of the outputs from off-line optimization strategies [11]. The performance with a constant $s_0$ were also evaluated in [13], leading to results close to the optimality.

Among the available options, a very robust approach consists of an equivalence factor correction, $s_{corr}$, depending on the current SoC [19]. The correction function is expressed as:

$$s_{corr}\left(SoC(t)\right) = \left[1 + \left(\frac{SoC_{target} - SoC(t)}{\Delta SoC}\right)^{2n+1}\right] \cdot$$
$$\left[1 + \tanh\left(\frac{f_{corr}\left(SoC(t)\right)}{p_{th}}\right)\right] \qquad (8)$$

$$f_{corr}\left(SoC(t)\right) = 0.99 f_{corr}\left(SoC(t-\Delta t)\right) + 0.01\left(SoC_{target} - SoC(t)\right) \qquad (9)$$

where $SoC_{target}$ and $\Delta SoC$ are a reference SoC level and its variation amplitude, $n$ is an integer (usually equal to 2 or 3), $p_{th}$ is the tolerance of the hyperbolic tangent function. The first factor represents a proportional correction term, whereas the second one is an integral correction. For the on-line optimization described in the next sections, this simple method is selected to realize the strategy adaptivity.

## Description of the Efficient Thermal Electric Skipping Strategy

The basic idea behind ETESS is an alternate utilization of the electric units and thermal engine to fulfill the power demand at the vehicle wheels, $P_{dem}$. The choice between the two modes depends, at each time, on the comparison between the actual consumption of the thermal engine, operating to fully satisfy the power demand, $\dot{m}_{f,th}$, and an equivalent fuel consumption, $\dot{m}_{f,el}$, associated to a pure electric driving of the vehicle. The basic concept for the identification of $\dot{m}_{f,el}$ is that, in a series mode, the power delivered by the EM to fulfill a certain power demand at the wheels, $P_{dem}$, was produced by the thermal engine in an undefined time, working in its optimal operating point, characterized by a $BSFC_{min}$. The power flux from the thermal engine to the wheel, in a pure series driving, involves some losses in the EG, in the EM, in the battery, in the GB2 and in the differential, which can be quantified by the efficiencies of each component. The equivalent fuel consumption in a pure electric mode is hence defined as the product of $P_{dem}$ and an "adapted" $BSFC_{min}$, which is corrected by the above-mentioned efficiencies to take into account the losses from the ICE to the wheels.

$$\dot{m}_{f,el} = c_0 \cdot \frac{P_{dem} \cdot BSFC_{min}}{\eta_{GB_2}\ \eta_{EG}\ \eta_{EM}\ \eta_{diff}} \qquad (10)$$

where $\eta_{GB2}$, $\eta_{EG}$, $\eta_{EM}$ and $\eta_{diff}$ are the efficiencies of GB2, EG, EM, and differential, respectively, and $c_0$ is tuning constant. Of course, some Joule losses occurs in the battery, but they are not directly considered in the $\dot{m}_{f,el}$ formulation to preserve its mathematical simplicity. The tuning constant $c_0$ is introduced to realize the energy balance for the battery, Eq. (6). The identification of the fuel consumption in a pure thermal engine driving only depends on the power demand, $P_{dem}$, and on the losses in the GB1 and in the differential, leading to the following definition:

$$\dot{m}_{f,th} = \frac{P_{dem} \cdot BSFC}{\eta_{GB_1}\eta_{diff}} \qquad (11)$$

where $\eta_{GB1}$ is the efficiency of GB1 and BSFC is the actual fuel consumption of the engine operating with the load and speed imposed by the vehicle velocity and by $P_{dem}$. For the evaluations of both $\dot{m}_{f,th}$ and $\dot{m}_{f,el}$, the only potential degree of freedom is the gear selection of the linked gearboxes. This is straightforwardly done choosing the one which leads to the lowest fuel rate.

Based on the above definitions, the strategy for the selection between pure electric and thermal engine driving can be summarized by the inequalities below:

$$\begin{cases} \dot{m}_{f,el} < \dot{m}_{f,th} \implies pure\ electric\ mode \\ \dot{m}_{f,el} > \dot{m}_{f,th} \implies pure\ thermal\ mode \end{cases} \qquad (12)$$

As a concise description of the ETESS principle, this strategy can be considered as a specialization of the ECMS, where the only allowed values for the power-split are either 0 or 1. The introduction of such simplification is expected to involve a certain penalization of the fuel economy, but, on the other hand, a drastic reduction of the computational effort.
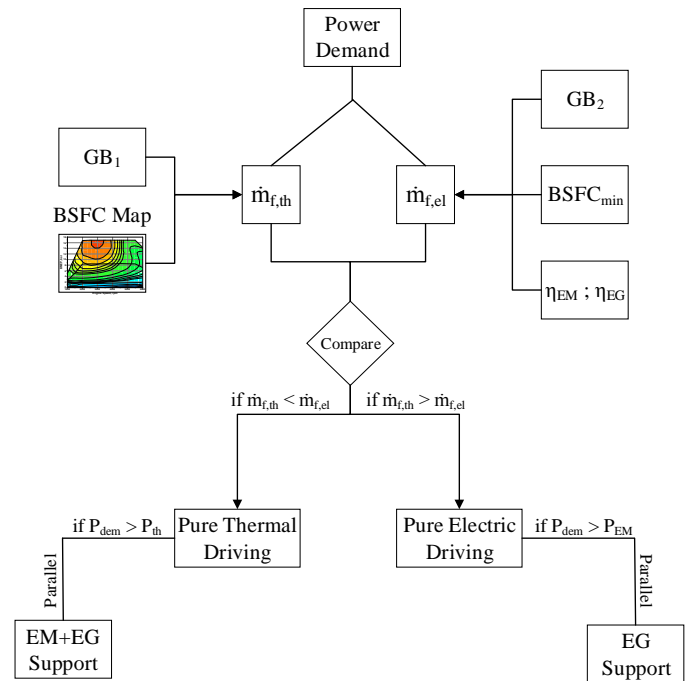


Figure 3. Flowchart schematizing the logics of the ETESS.

Coming back to the description of the ETESS logics, a hybrid driving is activated only when the thermal engine or the two combined electric units are not able to fully supply the vehicle power demand in an independent way. In this case, the ICE will work at the maximum rated power, while the electric units furnish the remaining power to fulfill the vehicle power demand. A regenerative braking is activated when the wheel power demand becomes negative, realized only by the EM or with the support of the EG, depending on the power to be recovered. To summarize the logics of the ETESS, a flowchart is presented in Figure 3. The latter highlights the choice between a pure electric or thermal driving, with the activation of a parallel mode only when the ICE or the EM are not able to fulfill alone the power demand.

Following the proposed approach, the battery charge is activated most likely during the vehicle decelerations and less frequently in a phase with a positive power demand. In this way, the energy flux from the thermal engine to the battery (throughout the electric units) is reduced as much as possible, minimizing the related unavoidable mechanical and electrical losses. If the torque constraints for both thermal and electric units are not exceeded along a driving cycle, the only energy available for a pure electric driving is the one recovered from the regenerative braking, and the thermal engine, when switched on, will supply the power strictly needed for the vehicle driving.

Based on the simple inequality of Eq. (12), the choice between pure electric or thermal engine driving is straightforward, without the need of the discrete map exploration. The engine operating point to be inquired for the evaluation of $\dot{m}_{f,th}$ is univocally determined by the tractive power demand, by the vehicle speed, by the losses along the driveline from the wheel to the engine. This evaluation has to be repeated only for the available gears of the gearbox linked to the thermal engine. Similarly, the fuel rate $\dot{m}_{f,el}$ in a pure electric driving is univocally determined, once again, by the traction power demand, by the vehicle speed, and by the losses along the driveline, and in addition by the dissipations in the electric units.

For the above reasons, the proposed approach involves a much-reduced computational effort compared to PMP, ECMS or GOS in general, not being needed any discrete map exploration. Anyway, the ETESS suffers from a drawback similar to the PMP ones, namely the need of a-priori knowledge of the speed-profile to select the value of $c_0$. However, it can be straightly extended to a real-time application introducing an adaptive correction for $c_0$, in a manner similar to the ECMS approach.

As final consideration, it is worth to underline that the proposed control strategy is versatile and suitable to any hybrid vehicle architecture. The application here described represents just an example for a quite complex test case.

## Assessment with a commercial tool

In a preliminary stage, the developed simulation tool (UNVS) and the logics implemented for hybrid vehicles are compared with a commercial software (tool HOT of Simcenter Amesim, V17.0) in order to test their consistency for a representative test case. To this aim, the HEV previously presented is simulated along a WLTC. The vehicle is schematized in both software, according to the data listed in Table 1 and to the BSFC map in Figure 2. In both cases, the ECMS with a constant equivalence factor is used to realize the powertrain management. No modification of the default parameters for the simulation settings is adopted in the commercial software (no penalizations at engine switch on/off and at mode change). The number of breakpoints for the exploration of the electric unit maps is unchanged from the default value (9 for both EM and EG). The same settings are selected in UNVS to get the maximum possible congruence. The time history of the main control and performance parameters along the driving cycle are plotted in Figure 4. Power profiles concerning the power delivered / absorbed by the thermal engine and by the electric units are in most cases superimposed. Moreover, the units are switched on/off very often at the same times.

For both software, all the units work in similar way, privileging an electric driving during the low-speed sections of the cycle and an ICE driving in the other parts. When a hybrid propulsion is activated (power-split), the UNVS seems to prefer a support from the EM to the thermal engine, while the commercial code involves a more relevant support from the EG.

Concerning the phases where the electric driving is privileged, HOT selects more frequently a power-split between the electric units. On the opposite, UNVS choses to supply the power demand mainly by the EM, and EG is activated only if necessary. Concerning the thermal engine, when it is switched on, in most part of the cycle, it is controlled to deliver alone the vehicle power demand. With reference to the developed simulation platform, the ICE produces a power surplus in very few periods, especially during the cycle portions where the speed is high (for instance, between 1180 and 1185 s). This is not the case of HOT, where the charging phases promoted by the engine are more homogenously distributed along the driving cycle. The regenerative braking, as expected, is mainly carried out by the EM, not being required the support of EG for the considered vehicle/cycle.

The described differences reflect on the SoC trends, with a flatter shape for HOT outcomes due to more frequent and homogenous charging phases. Despite of those differences, the global SoC trends are quite similar, confirming the consistency between the compared software. The instantaneous fuel rates follow the trends of the ICE power and minor differences emerge in the gear number selection.

The presented results highlight the substantial congruence between the physics and the control management implemented in the compared models, leading to a consumed fuel prediction, along the driving cycle, by UNVS lower than HOT of 2.4%. The disagreement in the handling of the charging phases is probably due to a different gridding rules of the operating domain of the thermal engine and electric units. Despite those incongruences, the management of the powertrain is globally similar, leading to reduced difference of consumed fuel. As a final consideration, this preliminary assessment demonstrates the reliability of the developed simulation tool, which will be employed in the next section to test the potential of the ETESS in comparison with PMP and ECMS.
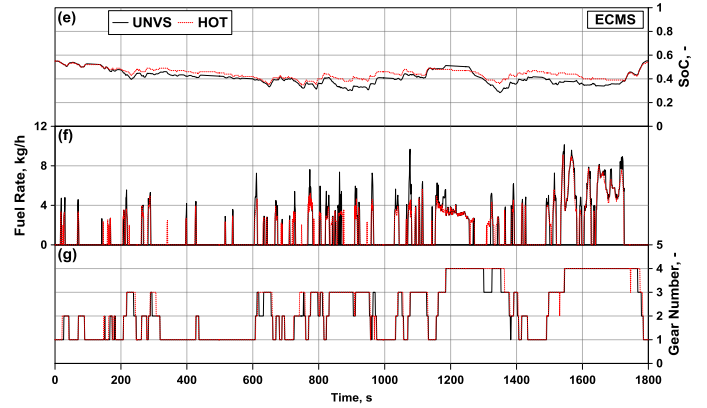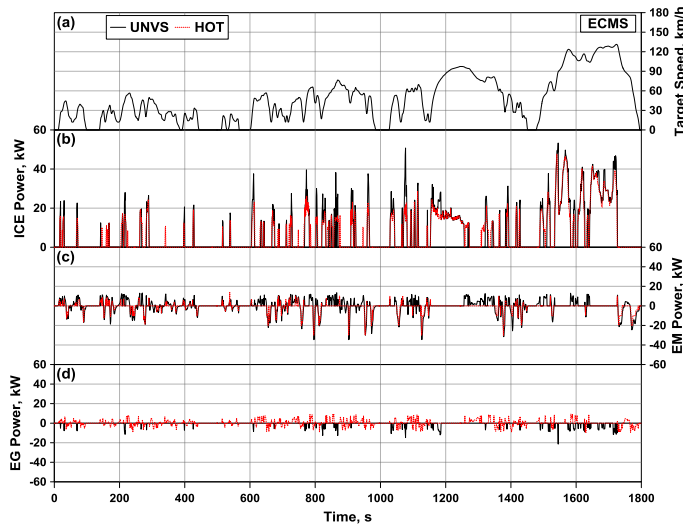
Figure 4. UNVS / HOT comparison of ICE power (b), EM power (c), EG power (d), SoC (e), fuel rate (f) and GB$_1$ number (g) along the WLTC (vehicle speed – (a)).

## Discussion of ETESS potential

In a first stage, this section describes the assessment between the ETESS and the PMP in off-line simulations, concerning the tested hybrid vehicle along different driving cycles and powertrain designs. All calculations are carried out by the UNVS to guarantee the maximum fair in the comparisons between the strategies. Depending on the driving cycle and on the powertrain design, the values of constant $\lambda^*$ and $c_0$ are tuned case-by-case to realize the battery energy balance between the cycle start and end. Table 2 collects the tested configurations, highlighting the driving cycle and the powertrain characteristics. Six driving cycles are considered and some variants of the powertrain. Cases from #1 to #6 refer to standardized speed missions (WLTC and Artemis variants), whereas cases #7 and #8 relate to RDE cycles. Their speed and altitude profiles are plotted in Figure 5 and their main data are collected in Table 3.

In Table 2, "Base" refers to the baseline performance, while "Red" indicates a motor or engine having reduced maximum and minimum torque, maintaining the same rotational speed range. In particular, the "Red" configuration involves performance halved for the thermal engine and equal to one fifth for the electric units. Finally, the last column, referring to the battery sizing, presents for the last two cases a doubled capacity ("Big"), adapted for the longer durations of the RDE cycles.

Table 2. Simulation raster.

| Case # | Driving cycle | ICE | EM | EG | Ba |
|---|---|---|---|---|---|
| 1 | WLTC | Base | Base | Base | Base |
| 2 | WLTC | Red | Base | Base | Base |
| 3 | WLTC | Base | Red | Red | Base |
| 4 | Artemis Motorway | Base | Base | Base | Base |
| 5 | Artemis Road | Base | Base | Base | Base |
| 6 | Artemis Urban | Base | Base | Base | Base |
| 7 | RDE1 | Base | Base | Base | Big |
| 8 | RDE2 | Base | Base | Base | Big |

Table 3. RDE main data.

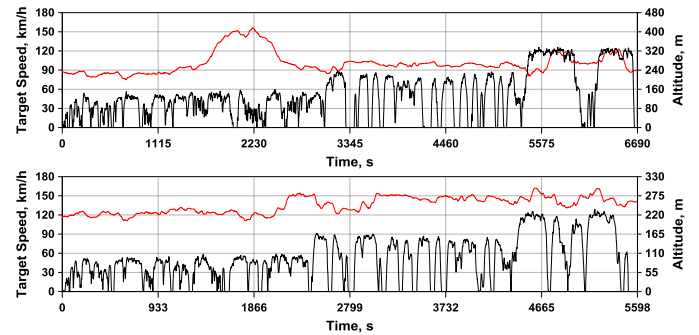| Case # | RDE1 | RDE2 |
|---|---|---|
| Length, m | 93'939 | 78'853 |
| Duration, s | 6'693 | 5'599 |
| Mean Speed, km/h | 56.2 | 56.3 |
| Max Speed, km/h | 126 | 129 |
| Mean Accel., m/s$^2$ | 0.39 | 0.41 |
| Max Accel., m/s$^2$ | 3.33 | 5.04 |
| Mean Decel., m/s$^2$ | -0.42 | -0.43 |
| Max Decel., m/s$^2$ | -3.14 | -3.38 |



Figure 5. RDE cycles target speed and altitude profiles.

All the simulations based on the PMP are carried out with a higher number of breakpoints compared to the one used in the preliminary calculations in the previous section (29 and 19 for EM and EG, respectively). Moreover, a certain hysteresis is introduced to limit the frequency of series/parallel mode switches. For sake of brevity, detailed results will be examined for cases #1, #2, #5 and #7.

Starting the discussion from the case #1, as can be seen in Figure 6 a-h, ETESS and PMP give almost superimposed results of EM, EG and ICE powers, which reflect on the trends of fuel rate, SoC and selected gear number. The hybrid mode trends (parallel (0) or series (1), in Figure 7h) are practically superimposed in most part of the cycle.
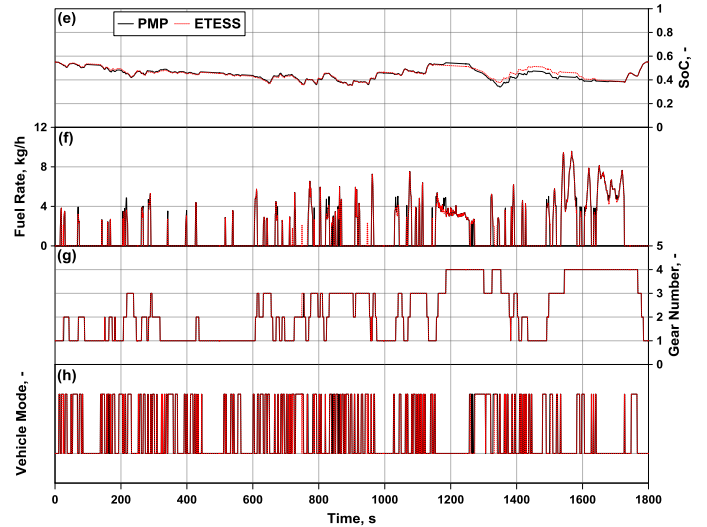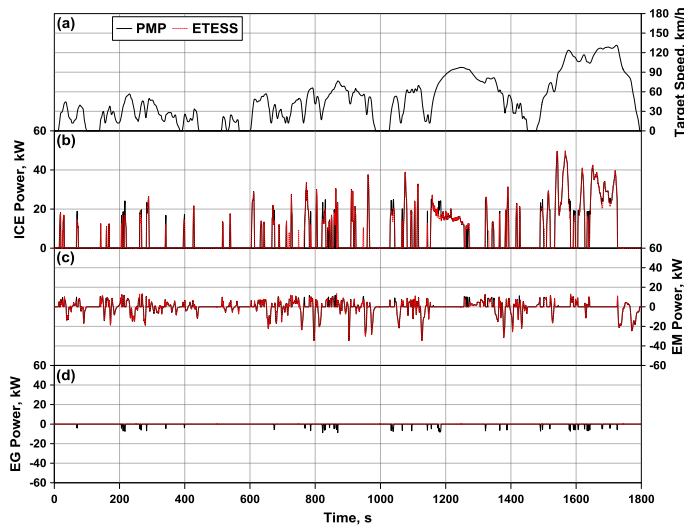
Figure 6. PMP/ETESS comparisons of ICE power (b), EM power (c), EG power (d), SoC (e), fuel rate (f), $GB_1$ number (g) and vehicle mode (h) along the WLTC (vehicle speed – (a)) – case #1.
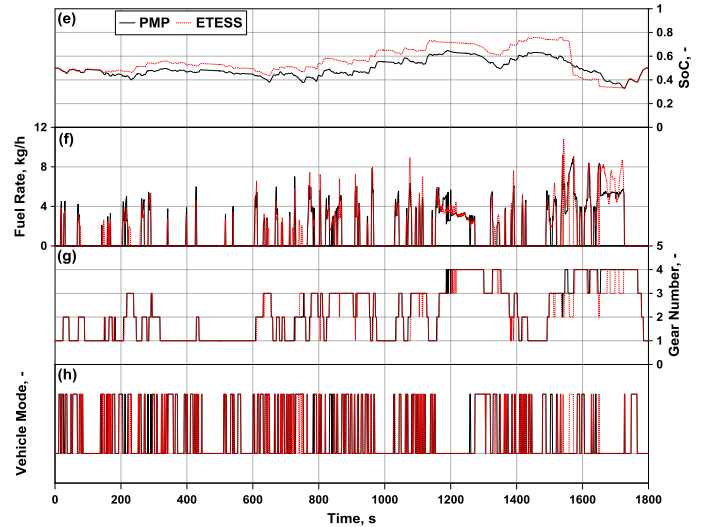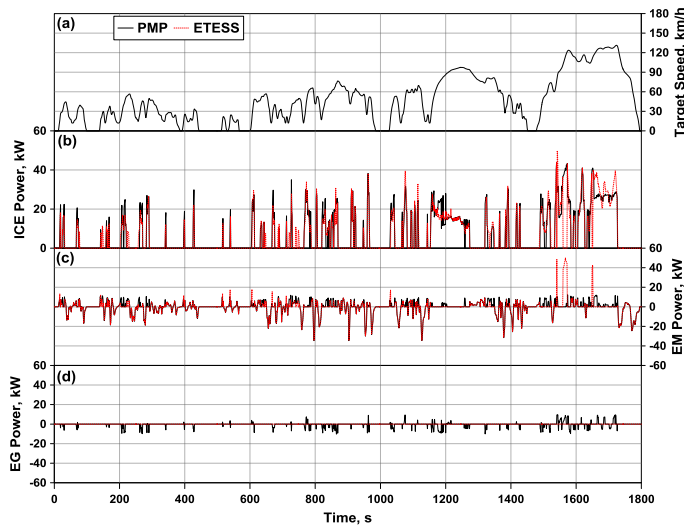


Figure 7. PMP/ETESS comparison of ICE power (b), EM power (c), EG power (d), SoC (e), fuel rate (f), $GB_1$ number (g) and vehicle mode (h) for a reduced torque engine along the WLTC (vehicle speed – (a)) – case #2.

In case #2, the vehicle architecture is modified by reducing the maximum ICE torque, corresponding to the BMEP dashed line in Figure 2. The BSFC map is not modified compared to the baseline engine. The comparisons in Figure 7 shows some differences between the PMP and ETESS, especially during the high-speed portion of the driving cycle (Figure 7a). Because of the reduced size of the thermal unit, the electric driving is selected by the ETESS even during the high-speed portion of the cycle (see around 1570 s), which reflects in a sudden SoC reduction. The PMP, thanks to the power-split application, allows a support to the ICE by the EM (see EM power in Figure 7c), and a more homogeneous battery charging along the cycle (see EG power in Figure 7d). The reduced ICE power also involve gear downshifts for the ETESS compared to the PMP during the last high-speed portion (for instance, between 1550 s and 1575 s - see Figure 7g), with the consequent fuel rate penalizations (Figure 7f). Further simulations are performed by using the baseline powertrain, changing the driving cycle. As said, for sake of brevity, only the comparisons for two Artemis driving cycles are reported below (case #5 and case #7). The first one, in Figure 8, concerns the Artemis MotorWay. This last is characterized by a higher averaged vehicle speed compared to the WLTC, with peaks up to 150 km/h.

Comparing ETESS and PMP, it can be seen that they give once again similar results for EM, EG and ICE powers (Figure 8b-c-d). In some cases (for instance between 840 and 848 s), the PMP determines a power-split between ICE and electric units, while ETESS selects a lower gear number (Figure 8g) to fulfil the power demand only by the ICE. This affects the SoC trend, where the ETESS involves a slightly lower level during the central portion of the cycle (Figure 8e), and on the fuel rate profile (Figure 8f). The second Artemis cycle here discussed is the Artemis Urban (Figure 9). Velocity target (Figure 9a) presents a lower averaged value and peak levels (around 60 km/h) compared to the MotorWay variant (Figure 8(a)), related to a general lower power demand for the powertrain. For the case #7, the PMP and the ETESS behaves in a very similar way for all the monitored parameters.

The detailed analysis of the instantaneous trends for the compared control strategies demonstrates their substantial coherence, with some differences only when the operating limits of thermal or electrical units are reached.
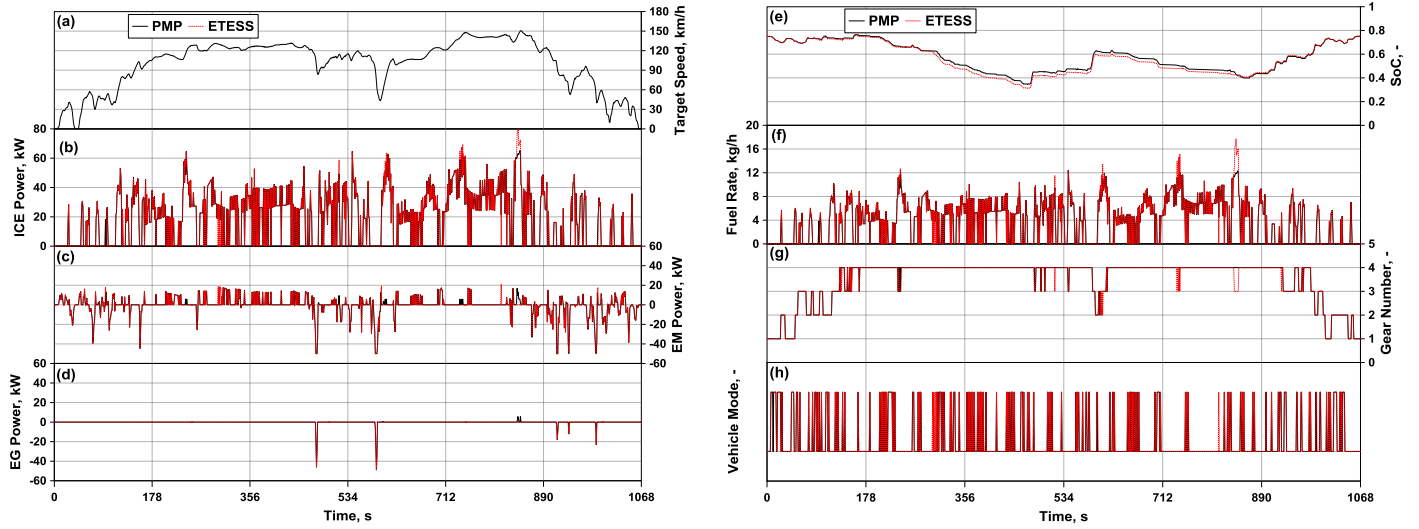
Figure 8. PMP/ETESS comparison of ICE power (b), EM power (c), EG power (d), SoC (e), fuel rate (f), GB1 number (g) and vehicle mode (h) along the Artemis MotorWay (vehicle speed – (a)) – case #5.
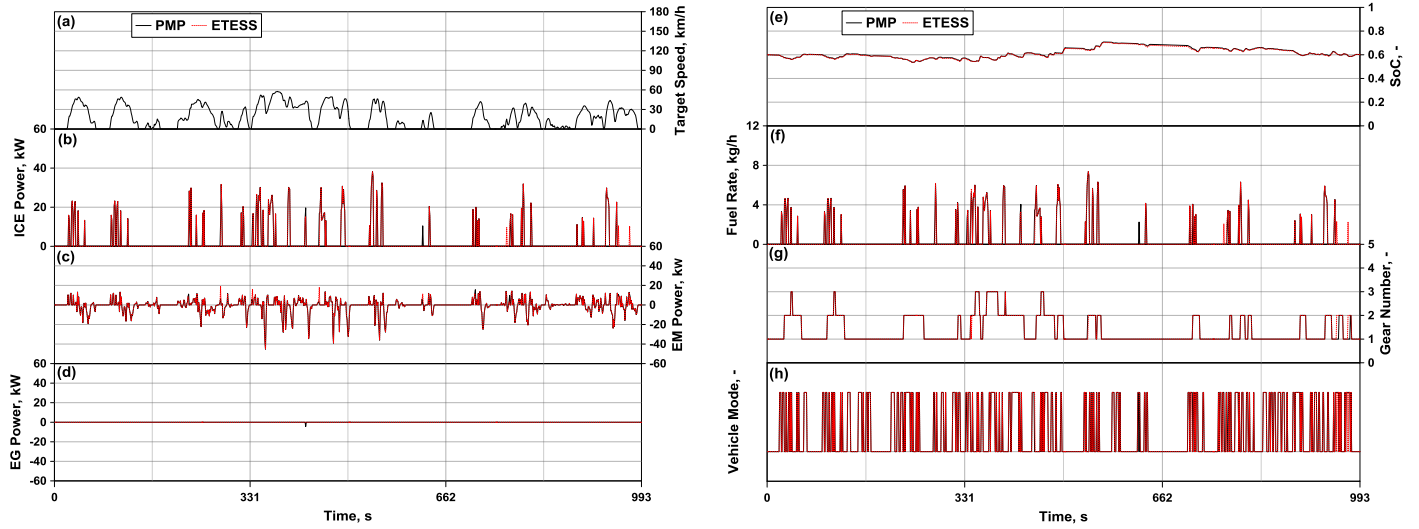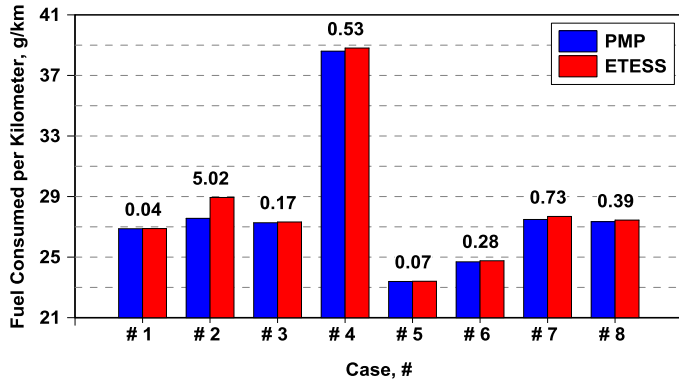


Figure 9. PMP/ETESS comparison of ICE power (b), EM power (c), EG power (d), SoC (e), fuel rate (f), $GB_1$ number (g) and vehicle mode (h) along the Artemis Urban (vehicle speed – (a)) – case #7.



Figure 10. Assessment between off-line ETESS and PMP of kilometric consumed fuel and percent difference in the cases of Table 2.

A global comparison between ETESS and PMP is realized by the bar charts in Figure 10. They represent the consumed mass of fuel per kilometer for all the considered tests, and over each couple of bars is shown the fuel consumption percent difference. The ETESS performs

in a way similar as PMP, with an average penalization of about 1% and, in most cases, below 0.5%. Greater differences emerge only for case #2, where more frequently the power limit of the thermal unit is reached, and the logics of ETESS fails, determining a far-from optimal control. On the other hand, simulations based on ETESS execute with a shorter computational time, with an advantage of 99 % on average. On the base of the above results, ETESS shows the potential for a real-time implementation.

The on-line variant of ETESS is tested introducing adaptative correction for the constant $c_0$, by the factor $s_{corr}$, Eq. (8). This multiplies a case-independent constant $\bar{c}_0$, which is obtained by the average of the case-by-case tuned values derived from the above presented analyses. The on-line simulations are repeated for all the cases in Table 2 and the results are compared to the ones from ECMS. For the ECMS, the equivalence factor adaptivity is realized multiplying a constant, once again, by the correction factor expressed by Eq. (8). In a manner similar to the adaptive ETESS, the constant value is obtained as an average of case-by-case tuned $s_0$ values found in preliminary simulations in off-line mode for all cases in Table 2.

This methodology is chosen to test the robustness of the on-line ETESS for different vehicle variants and driving missions. To preserve the assessment consistency, an analogous method is followed for the definition of the adaptive ECMS equivalence factor.

The on-line optimizations involve 6 simulations for each case, with different initial SoC and the same final target. As an example, in Figure 11, the SoC traces are shown for the case #1. The results of those analyses are combined, according to the WLTP procedure [20], to extract a corrected kilometric fuel consumption. The results are collected in the bar chart in Figure 12. The ETESS gives results very close to ECMS, confirming the robustness of the methodology. A fuel consumption penalization of slightly lower than 1 % emerges on average. ETESS gives substantially worse performance than ECMS only in the case #2, while works even better in the case #1. The advantages in the simulation time are confirmed in on-line ETESS variant in the comparison with the ECMS.

As a final consideration, the performance worsening of ETESS compared to widespread methodologies (PMP and ECMS) appear reasonable in the light of its computational efficiency. This demonstrates the potential for a real-time implementation. The strategy shows a certain robustness, under different vehicle configurations and driving missions.

The future developments of this activity will regard a more efficient handling of operations with the thermal engine working close to its power/torque limits. Moreover, the consistency of the ETESS will be verified in cases of more complex modelling of some powertrain sub-components (for instance, variable efficiencies of electric units, gearbox and battery) and in a dynamic forward simulation.
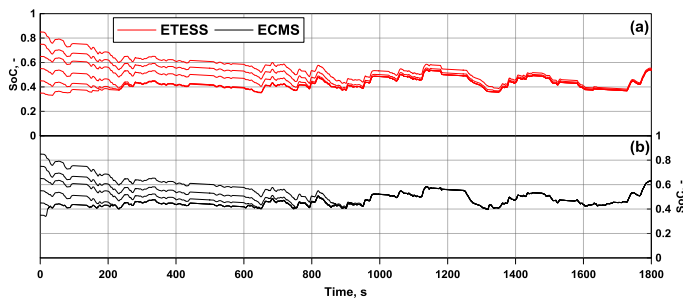


Figure 11. Representative SoC trends for the ETESS (a) and ECMS (b) for different initial SoC values, case #1.
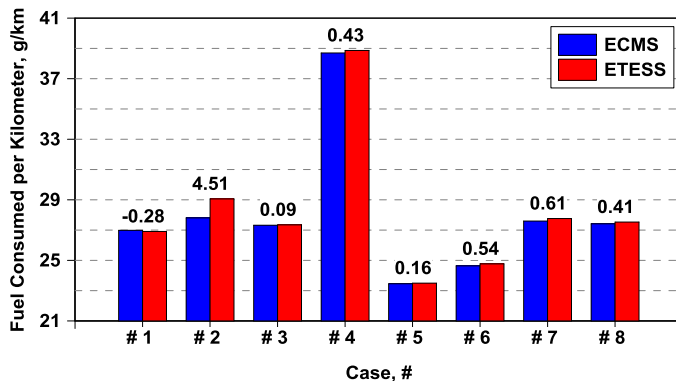


Figure 12. Assessment between on-line ETESS and ECMS of kilometric consumed fuel and percent difference in the cases of Table 2.

## Conclusions

This paper describes a simplified control strategy for hybrid vehicles, named ETESS. It is applied to a series/parallel combined powertrain, installed on a segment C vehicle. This strategy is implemented in a model developed in a "in-house" code. The basic concept of the ETESS is an alternate utilization of thermal and electric units to fulfill the power demand of the vehicle. Conversely to the most common strategies, based on the power-split concept, a simultaneous activation of all units is allowed only when the operating constraints of one of them are reached.

In a preliminary stage, the simulation tool is assessed with a commercial software, proving a substantial congruence between the numerical approaches. Then, a simulation raster is arranged to compare the ETESS with the well-know PMP approach. To test the robustness and versatility of the proposed strategy, various driving cycles and powertrain architectures are considered.

Off-line simulations point out that ETESS involves a reduced penalization of the fuel economy compared to PMP (increase of about 1 % on average), but a drastically reduced computational effort (99% decrease on average). Major fuel consumption differences emerge in the tests with reduced power of the thermal unit, where the logics of ETESS fails.

The consistency of the ETESS is tested by on-line simulations, to verify the possibility to be used in a real-time vehicle application. To this aim, a comparison with ECMS approach is realized. The results confirm that the on-line variant of ETESS performs in a way similar to ECMS, with a fuel consumption penalization slightly lower than 1% on average. Once again, the main advantage is a drastically reduced calculation effort.

As a future development, the proposed control strategy will be refined to improve the performance when electric and/or thermal units of the powertrain attain their operating limits. Moreover, ETESS will be tested in more complex simulation frameworks (variable electric unit efficiency and components dynamics) and with more stringent limitations on ICE switch on/off frequency.

## Acknowledgements

## Contact information

## References

1. Morita, K., "Automotive power source in 21st century," *JSAE Review* 24(1):3-7, 2003, doi: 10.1016/S0389-4304(02)00250-3.
2. Guzzella, L., Sciarretta, A., "Vehicle propulsion systems: introduction to modeling and optimization," (Berlin, Springer-Verlag, 2013), doi: 10.1007/978-3-642-35913-2.
3. Patil, R. M., Filipi, Z., Fathy, H. K., "Comparison of Supervisory Control Strategies for Series Plug-In Hybrid

Electric Vehicle Powertrains Through Dynamic Programming," *IEEE Transactions on Control Systems Technology* 22(2):502-509, 2014, doi: 10.1109/TCST.2013.2257778.

4. Brahma, A., Guezennec, Y., Rizzoni, G., "Optimal energy management in series hybrid electric vehicles," *Proceedings of the 2000 American Control Conference* 1(6):60-64, 2000, doi: 10.1109/ACC.2000.878772.

5. Lin, C., Peng, H., Grizzle, J., Liu, J. et al., "Control System Development for an Advanced-Technology Medium-Duty Hybrid Electric Truck," SAE Technical Paper 2003-01-3369, 2003, doi: 10.4271/2003-01-3369.

6. Moura, S.J., Fathy, H.K., Callaway, D.S., Stein, J.,L., "A Stochastic Optimal Control Approach for Power Management in Plug-In Hybrid Electric Vehicles," *IEEE Transactions on Control Systems Technology* 19(3): 545-555, 2011, doi: 10.1109/TCST.2010.2043736.

7. Kim, N., Cha, S., Peng, H., "Optimal control of hybrid electric vehicles based on Pontryagin's minimum principle," *IEEE Transactions on Control Systems Technology* 19(5):1279-1287, 2011, doi: 10.1109/TCST.2010.2061232.

8. Paganelli, G., Delprat, S., Guerra, T. M., Rimaux, J., Santin, J. J., "Equivalent consumption minimization strategy for parallel hybrid powertrains," *Vehicular Technology Conference IEEE 55th Vehicular Technology Conference VTC Spring 2002* 4:2076-2081, 2002, doi: 10.1109/VTC.2002.1002989.

9. Sciarretta, A., Guzzella, L., "Control of hybrid electric vehicles," *IEEE Control Systems Magazine* 27(2):60-70, 2007, doi: 10.1109/MCS.2007.338280.

10. Zhang, F., Xi, J.Q., Langari, R., "An adaptive equivalent consumption minimization strategy for parallel hybrid electric vehicle based on Fuzzy PI," *Proceeding of 2016 IEEE Intelligent Vehicles Symposium (IV)* 460-465, 2016, doi: 10.1109/IVS.2016.7535426.

11. Pei, D., Leamy, M. J., "Dynamic Programming-Informed Equivalent Cost Minimization Control Strategies for Hybrid-Electric Vehicles," *J. Dyn. Sys., Meas., Control* 135(5):051013, 2013, doi: 10.1115/1.4024788.

12. Serrao, L., Onori, S., Rizzoni, G., "A comparative analysis of energy management strategies for hybrid electric vehicles," *J. Dyn. Sys., Meas., Control* 133(3):031012, 2011, doi: 10.1115/1.4003267.

13. Musardo, C., Rizzoni, G., Guezennec, Y, Staccia, B, "A-ECMS: An Adaptive Algorithm for Hybrid Electric Vehicle Energy Management", *European Journal of Control* 11(4-5): 509-524, 2013, doi: 10.3166/ejc.11.509-524.

14. Tufano, D., De Bellis, V., Malfi, E., "Development of an on-line energy management strategy for hybrid electric vehicle," Energy Procedia 148: 106-113, 2018, doi: 0.1016/j.egypro.2018.08.037.

15. Bozza, F., Tufano, D., Malfi, E., Teodosio, L. et al., "Performance and Emissions of an Advanced Multi-Cylinder SI Engine Operating in Ultra-Lean Conditions," SAE Technical Paper 2019-24-0075, 2019, doi: 10.4271/2019-24-0075.

16. Valera, J. J., Iglesias, I., Peña, A., Martín, A., Sánchez, J., "Integrated Modeling Approach for Highly electrified HEV. Virtual Design and Simulation Methodology for Advanced Powertrain Prototyping," *World Electric Vehicle Journal* 3(4):694-701, 2009, doi: 10.3390/wevj3040694.

17. Dekraker, P., Barba, D., Moskalik, A., and Butters, K., "Constructing Engine Maps for Full Vehicle Simulation Modeling," SAE Technical Paper 2018-01-1412, 2018, doi:10.4271/2018-01-1412.

18. Mock, P., Kühlwein, J., Tietge, U., Franco, V., Bandivadekar, A., German, J., "The WLTP: How a new test procedure for cars will affect fuel consumption values in the EU", Working Paper 2014-9, https://theicct.org/publications/wltp-how-new-test-procedure-cars-will-affect-fuel-consumption-values-eu, accessed Nov. 2019.

19. Koprubasi, K., "Modeling and control of a Hybrid-Electric Vehicle for Drivability and Fuel Economy Improvements", Ph.D. Thesis, The Ohio State University, 2008.

20. Commission Regulation EU, 2018/1832 of 5 November 2018, Official Journal of the European Union L 301/1, https://eur-lex.europa.eu/legal-content/EN/TXT/PDF/?uri=CELEX:32018R1832&from=FR, accessed Nov. 2019.

## Acronyms

| | |
|---|---|
| **Cl** | Clutch |
| **Ba** | Battery |
| **BMEP** | Brake mean effective pressure |
| **BSFC** | Brake Specific Fuel Consumption |
| **DP** | Dynamic Programming |
| **ECMS** | Equivalent Consumption Minimization Strategy |
| **ETESS** | Efficient Thermal Electric Skipping Strategy |
| **EM** | Electric Motor |
| **EG** | Electric Generator |
| **GB** | Gear-Boxes |
| **GOS** | Global Optimization Strategy |
| **HEV** | Hybrid electric vehicle |
| **ICE** | Internal combustion engine |
| **LHV** | Lower heating value |
| **NEDC** | New European Driving Cycle |
| **PI** | Proportional-Integrative |
| **PMP** | Pontryagin minimum principle |
| **RDE** | Real Driving Emission |
| **SI** | Spark ignition |
| **SoC** | State of Charge |
| **UNVS** | UniNa Vehicle Simulation |
| **WLTC** | Worldwide harmonized Light-Duty vehicles Test Cycle |
| **WLTP** | Worldwide harmonized Light-Duty vehicles Test Procedure |

## Symbols

| | |
|---|---|
| $c_0$ | Tuning constant |
| $f$ | Function |
| $H$ | Hamiltonian |
| $J$ | Performance index |
| $L$ | Cost function |
| $m$ | Mass |
| $P$ | Power |
| $p_{th}$ | Tolerance of the hyperbolic tangent function |
| $s_0$ | Equivalence factor |
| $s_{corr}$ | Equivalence factor correction |
| $t$ | Time |
| $u$ | Control variable, power-split |
| $U$ | Variation range of the control variable |
| $x$ | State variable |
| $X$ | Variation range of the state variable |

## Greeks

| | |
|---|---|
| $\beta$ | Penalization factor |
| $\eta$ | Efficiency |
| $\lambda$ | Costate |

## Subscripts

| | |
|---|---|
| $0$ | Initial |
| *batt* | Battery |

| | |
|---|---|
| *corr* | Correction |
| *dem* | Demand |
| *diff* | Differential |
| *el* | Electric |
| *eq* | Equivalent |
| *f* | Final, fuel |
| *min* | Minimum |
| *th* | Thermal |

## Superscripts

| | |
|---|---|
| **.** | Temporal derivative |
| * | Optimal |